02 May 2013, 4:00 pm - 6:00 pm

Improvement of Dynamic Soil Properties Induced by Preloading Verified by a Field Test and Embankment Failure

K. Stamatopoulos
Stamatopoulos and Associates Co., Greece

P. Petridis
Stamatopoulos and Associates Co., Greece

P. S. Allkja
ALTEA & Geostudio 2000, Albania

G. Vatselas
GeoSTAND Co., Greece

A. Small
ITM Limited, UK

Commemorate the Legacy of Ralph B. Peck
April 29 - May 4, 2013 CHICAGO
Seventh International Conference on
Case Histories in Geotechnical Engineering
and Symposium in Honor of Clyde Baker

IMPROVEMENT OF DYNAMIC SOIL PROPERTIES INDUCED BY PRELOADING VERIFIED BY A FIELD TEST AND EMBANKMENT FAILURE

K. Stamatopoulos, P. Petridis,
Stamatopoulos and Associates Co,
Athens, Greece
e-mail: info@saa-geotech.gr.

P. S. Allkja
ALTEA & Geostudio 2000,
Tirana, Albania

G. Vatselas
GeoSTAND Co
Athens, Greece

A. Small
ITM Limited
East Sussex , UK

ABSTRACT

The results of an elaborate field preloading study on a liquefaction-susceptible site are presented. Preloading was applied by a temporary embankment 9m high. Prior and after preloading, borings with standard penetration tests, cone penetration tests and geophysical studies were performed. During the process of embankment construction and demolition, settlements, excess pore pressures and vertical and horizontal stresses were recorded versus time at different locations. A partial embankment failure occurred during the preloading process. A method predicting failure during the construction of the preload embankment based on excess pore pressure measurements is proposed and verified.

INTRODUCTION

Preloading is a temporary loading, usually a soil embankment, applied at approximately level ground to improve subsurface soils by densification and increasing lateral stress (Alonso et al., 2000, Al-Shamrani and Dhowian, 1997, Stamatopoulos and Kotzias, 1885, Petridis et al, 2000). The method is frequently used to improve poor soil conditions and sustain large static loads. Many cases have been reported where the effectiveness of preloading has been demonstrated (Stamatopoulos and Kotzias, 1885, Petridis et al, 2000): For a height of the temporary soil embankment between about 7-13m, preloading-induced settlement of the order of tens of centimeters, that illustrates soil densification, was measured. In addition, construction after preloading was successful in terms of static settlements. Furthermore, the blow count measured with the Standard Penetration Test, SPT, versus depth was measured in some sites both before and after soil improvement, illustrating the improvement.

Most applications of preloading in the field include measurements of settlement at some locations during the preloading process and geotechnical investigations after preloading to verify soil improvement, without studying the effect of preloading on dynamic soil properties. The liquefaction cyclic strength is a critical soil parameter because it determines whether a site will liquefy under a design earthquake. Liquefaction is not allowed in building codes (European Standard, 2003). As a result of the difficulty of undisturbed sampling of sandy soils, the in-situ liquefaction cyclic strength is mainly estimated by field tests: the Standard Penetration Tests, SPT, the Cone Penetration Tests, CPT) and the shear wave velocity, Vs (Boulanger and Idriss, 2006, European Prestandard, 1994, European Standard, 2003, Idriss and Boulanger, 2004, Ishihara, 1993, Seed and De Alba, 1986). The effect of preloading on the cyclic liquefaction strength has been studied and demonstrated in the laboratory by performing cyclic triaxial and shear tests on reconstituted samples and empirical expressions predicting this increase have been proposed (Stamatopoulos et al., 2012, Stamatopoulos and Stamatopoulos, 2007). In addition, to the liquefaction cyclic strength, the shear wave velocity is a critical dynamic soil property. It determines the dynamic response of soils (Schnabel et al, 1972, Kramer, 1996). The effect of the void ratio, the confining stress and the stress history on the shear wave velocity has been studied in the laboratory by performing cyclic laboratory tests and empirical expressions predicting this increase have been proposed (Hardin, 1978, Kramer, 1996).

A field test with extensive measurements is the most efficient method to investigate the effect of preloading in changing the dynamic properties and increasing the cyclic liquefaction strength of soils in-situ. The reason is that field tests can illustrate (a) the improvement in the field, not only in terms of the in-situ soils and preloading characteristics, but also in

terms of measured in-situ changes in horizontal stress and void ratio, (b) the ability of predictive methods to predict the measured response and improvement, and (c) manner and rate that preloading should be applied in the field.

Only one field study where the increase in dynamic soil properties and quantities affecting them was found in the literature (Stamatopoulos et al., 2005, Raptakis, 2012): The preload embankment was 9m high. Soil resistance was measured before and after preloading in the field by Standard Penetration Tests and Cone Penetration Tests (CPT). The shear wave velocity resistance (Vs) was also measured before and after preloading in the field. The increase in horizontal stress caused by preloading was also measured (Stamatopoulos et al., 2005). This is important as increases in confining (octahedral) stress can be associated with increased liquefaction resistance (Ishihara and Takatsu, 1979). However, the site up to 10m depth consisted mainly of clay soil, and thus was not liquefaction-susceptible. Thus the measured increases in the N value of the SPT, the qc value of the CPT, the Vs and horizontal stress could not be associated with increases in liquefaction resistance. Furthermore, the vertical strain versus depth was not measured. This is a critical measurement, because it can correlate the change in dynamic properties of soil layers with the change in void ratio.

According to the above, a complete field test on a liquefaction-susceptible site with data of (a) the SPT and CPT strength and Vs versus depth before and after preloading and (b) changes in the horizontal stress and void ratio of the soil as a result of preloading does not exist in the literature and is needed to assess the effect of preloading in the dynamic soil properties and liquefaction risk and the ability of methods to predict this effect. Such a field test was performed recently during a project funded by the European Union.

Below, the field test performed and the measured change in dynamic and other soil properties is described. Then, a method predicting the risk of failure during construction of a preload embankment is given and evaluated based on the field test partial failure during construction.

THE FIELD TEST

Site

The site for the field test was in Porto Romano, 10km North of Durress in the Albanian coast (Fig. 1). The site was rented and four borings to 15m depth each with sampling and Standard Penetration Tests (SPT) every meter were performed to verify that the site is suitable for the purpose of the present research: (a) Poor soil conditions, (b) predominately sand or silt with Plasticity Index less than 10%, (c) shallow ground water. Then four soil additional borings 5m depth each with sampling and Standard Penetration Tests (SPT) every meter were performed at locations corresponding to distances less than 6.5m from the centre of the embankment to be built. Piezometers were installed in two borings to measure the elevation of the water table. A standard laboratory testing program including classification, compressibility and strength tests was also performed. In addition, three Cone Penetration Tests (CPT) soundings to 15 m depth each, and down-hole surveys for measuring the shear wave velocity (Vs) were performed. Fig. 2a gives the initial and maximum past vertical effective stress versus depth, estimated from oedometer tests. Fig. 3 gives the average (i) N value measured in the SPT, (ii) qc value measured in the CPT and Vs measurements versus depth. Table 1 gives the soil layers that exist in the site and their average plasticity index and fines content based on classification tests, as well as their compressibility estimated from oedometer tests. Average water table line was measured at depth 1m. Table 2 gives the average measured N_{SPT} , qc and Vs in all in-situ soil layers of table 1

Instrumentation

The following instruments were placed at the location of the field test, prior to construction of the preload embankment and worked properly: (a). Vertical pressure cells were installed just below the ground surface and at three locations that corresponded to different points from the centre to the edge of the embankment to be built. Figs 4 and 6 give the detailed locations of these instruments. (b) Horizontal pressure cells were placed at 5 locations that corresponded to distances 6.5 and 16.5m from the centre of the embankment and at depths of approximately 3, 6 and 12m. They were directed in a manner to estimate the radial horizontal stress. Figs. 4 and 6 give the detailed locations of these instruments. (c) In each horizontal cell location, pore pressure transducers were also installed in order to measure the excess pore pressure, and from the horizontal stress and excess pore pressure to extract the effective horizontal stress. Other pore pressure transducers were also installed at depths of approximately 3, 6 and 12m. Figs. 4 and 6 give the detailed locations of these instruments. (d) A horizontal Inclinometer was installed in level ground, along a radius of the embankment-to-be-constructed to measure the ground settlement versus time and horizontal location from the centerline of the conical embankment. (e). A magnetic extensiometer was installed very near the center of the base of the embankment-to-be-constructed to measure the ground displacement versus time and depth. In particular, the magnetic extensiometer measures the incremental displacement at 2m increments at depths 0 to 20m. (f) Settlement plates were placed near ground level at different locations of the embankment base to measure the settlement by topographic means, to verify the settlement measured by the other means. In particular, the five settlement plates were placed at locations that corresponded to different points from the centre to the edge of the embankment, in two vertical to each other directions. Fig. 4 gives the detailed locations of these instruments. The measurements of all the above instruments, except from the settlement plates, were taken electronically. All theses instruments were connected to a data logging system.

Embankment construction and demolition

A 50m diameter fill, 9m high and 13 m diameter at the crest truncated-cone-shaped preload earth fill was constructed . A

ramp was also constructed in order to perform construction. Construction started on 6/6/2011. This date corresponds to day 0 in all the graphs and days given below. The soil used to construct the embankment was sandy. Compaction of the layer was performed with a vibrator. Field density tests were performed to verify compaction and illustrate that the unit density of the soil was 2.03t/m3.

During the placement of the preload embankment, a slide occurred, presumably due to excess rate of construction on 24/6/2011 (day 18). Figs. 1b give representative photographs at the top and base of the embankment respectively. Figs. 4b give a schematic illustration and a topographic imprint of the failure. Fortunately, the instruments were not damaged during the slide, as they were located in regions not affected by the slide. In addition, this slide provided interesting data regarding the correct rate of construction of preloading embankments when a soft clay layer exists on shallow depths.

After the slide, part of the embankment was demolished and reconstructed. Construction continued at a considerably slower rate. Construction terminated, after reaching an embankment height of 9m from ground level after settlement, that corresponds to 8.54m above unsettled ground level, on 10/8/2011, or day 66. Fig. 1c gives a photograph of the embankment at top height. Fig. 4c gives a cross-section of the embankment at top height. The location of some instruments is also given in the figure. The embankment stayed until 10/10/11, or 126 days after the start of construction, or 60 days after construction. Then, the rate of settlement was very small, less than 0.001m/day. The embankment was removed in 11 days. Fig.5 gives the height of the embankment and the corresponding construction rate, both versus the days from the start of construction.

Instrument measurements and discussion

Fig. 6a gives the measured vertical stress induced by the preload embankment, both in terms of time and location. It can be observed that its change in terms of time follows the change in embankment height in terms of time. Table 3 gives the measured maximum vertical stress versus distance from the center of the cone.

Regarding settlement measurements, it was first observed that settlement measurements of all devices (horizontal inclinometer, magnetic extensiometer, settlement plates) were consistent with each other. Fig. 6b gives the settlement versus time in terms of location measured by the inclinometer. Fig. 2c gives the measured maximum and final settlement versus distance from the center of the cone. Table 4 gives the measured maximum and final settlement in terms of the distance from the centerline. Fig. 2b gives the variation of vertical strain with depth.

In the field test, ground settlement was large, about 0.6m, illustrating the considerable level of densification, or ground improvement. Regarding the variation of vertical strain with depth it can be observed that the vertical strain is maximum at the location that the soft clay layer (0-3.7m) and equals 10%. This is reasonable, as this layer (i) is near the surface and thus receives larger vertical stress from the preload embankment, (ii) is not preloaded and (iii) and has a large coefficient of compressibility, larger than the other layers that are sandy or silty. It should be noted that at the depths 1 to 1.5m the vertical strain is less, presumably because the soft clay material was replaced by the sandy soil from the preload embankment at these depths due to the settlement of the embankment and the slide that occurred during construction described above. At depth below 3.7m the vertical strain is reduced to about 1%.

The measured magnitude of settlement and the variation of settlement with the distance from the centreline were similar to previous preload applications (Stamatopoulos et al., 2005, Stamatopoulos and Kotzias, 1985). The time required for the soil to settle is also a critical factor in applications of preloading. The reason is delays in construction are sometimes very important for the project owner. The study illustrated that the preload procedure, including the generation of the ground settlement (i.e. the settlement rate to decrease to values less than 0.001m/day) occurred rather quickly, less than five months after the start of preload construction, even though a clay layer of 3.7m width existed in the ground surface. This is similar with observations of previous field tests in sites containing a considerable amount of sandy material (Stamatopoulos and Kotzias, 1885, Petridis et al, 2000, Stamatopoulos et al., 2005).

Fig. 6c gives the pore pressure both in terms of time and location measured by the pore pressure transducers. It can be observed that significant excess pore pressures occur only in devices at depths 2.5-3.2m. In devices in depths 5.9-11.7m excess pore pressures are very small. This is consistent with the soil layers at the site, as, according to table 1, only until a depth of 3.7m clayey soil exists. The other devices are in sandy or silty material, and thus consolidation occurs almost instantaneously and considerable excess pore pressures are not generated. Furthermore, at depths 2.5-3.2m it can be observed that the maximum excess pore pressures occurred when the rate of embankment construction was maximum, and more specifically just prior to the failure of the embankment. This explains failure, as described in detail below.

Due to disturbance as a result of instrument placement, the initial measurement of horizontal stress is not reliable. Thus, only the measured change of horizontal stress due to embankment construction and demolition is considered. Fig. 6d gives the measured change in effective horizontal stress in terms of time and device. It can be observed that the measured response of horizontal stress follows that of load application: When loading is applied, the increase in horizontal stress is almost immediate and follows that of the curve of load application. During constant load application, horizontal stress did not change considerably. When load was removed, the response was similarly quick to load removal, and a reduction in the horizontal stress was observed in most cells. After

removal of the surcharge, some horizontal stress remained and stayed more or less constant with time. Table 5 gives the measured maximum and final increase in horizontal stress due to embankment construction, Δσh-max and Δσh-res versus depth and distances 6.5 and 16.5m from the centerline. The measurements indicate that the increase in lateral stress ratio as a result of the preloading process varies between 0.9 and 0.1. The large value corresponds to depths 0-3.7m, while the small values correspond to larger depths where the OCR value induced by the surcharge was smaller.

Post-Improvement geotechnical investigations

After the performance of the field test identical to the pre-improvement field investigations were performed in order to investigate the post-improvement soil properties. Post-improvement geotechnical investigations were performed at a distance less than 2m from the corresponding locations of pre-improvement geotechnical investigations. Fig. 3 gives the average after soil improvement N value of the SPT, qc value of the CPT and Vs measurements versus depth. It can be observed that in almost all SPT, CPT, Vs separate locations versus depth, post-improvement values are larger than the corresponding pre-improvement values. Table 2 gives the average measured N_{SPT} , qc and Vs before and after soil improvement in all in-situ soil layers of table 1 and the corresponding ratio of increase. It can be observed that the maximum increase occurs at the upper soft layer. This is presumably a result of the maximum OCR value induced by preloading, in combination with minimum initial strength at this layer.

Increase in dynamic soil properties

Based on the pre- and post- improvement shear wave velocity versus depth given in Fig. 3, table 2 gives the measured increase in shear wave velocity per soil layer. It can be observed that the shear wave velocity increased from a factor of about 2 to a factor of about 1.1. The large value corresponds to depths 0-3.7m where soft clay exists, while the small values correspond to larger depths and denser layers.

Under earthquakes, the lower two layers of table 1 are susceptible to liquefacti considerable plasticity, liquefaction. For the sil CPT resistance the liqu using the state-of-the-ar Boulanger (2004). Base European Prestandard (1 layer, the liquefaction cy the SPT, according to (2006). Table 7 gives measurement used, for cyclic liquefaction stren 7m increased from 0.39- addition the cyclic liqu layer at depth 7-15m inc 13%. It can be observe produce similar results.

consistent with the non-homogeneous characteristics of soils and the different methods applied.

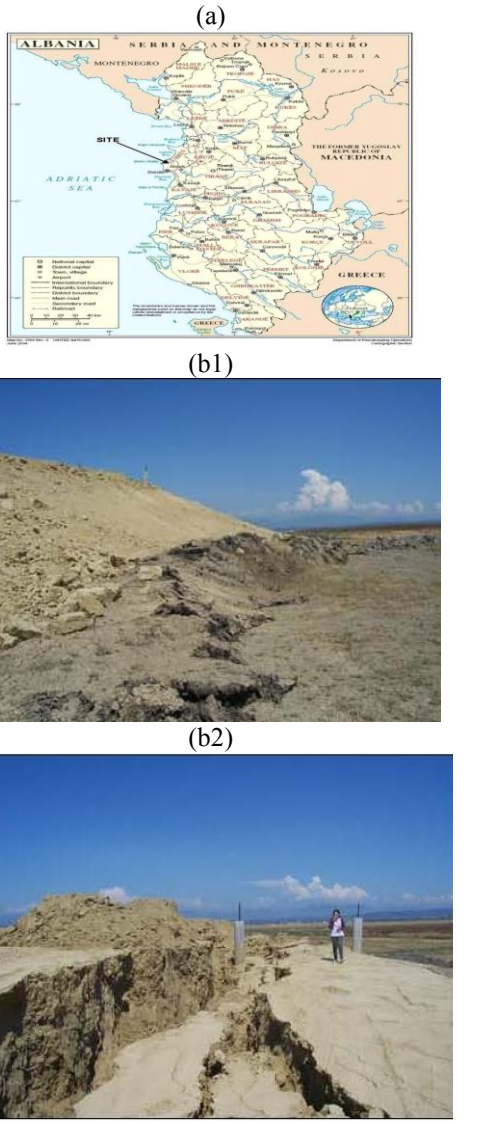

Fig. 1. Porto Romano field test. (a) General location of the site, (b) Photographs illustrating the failure of the embankment at day 18 from the start of construction, (c) Photograph of the embankment at top height

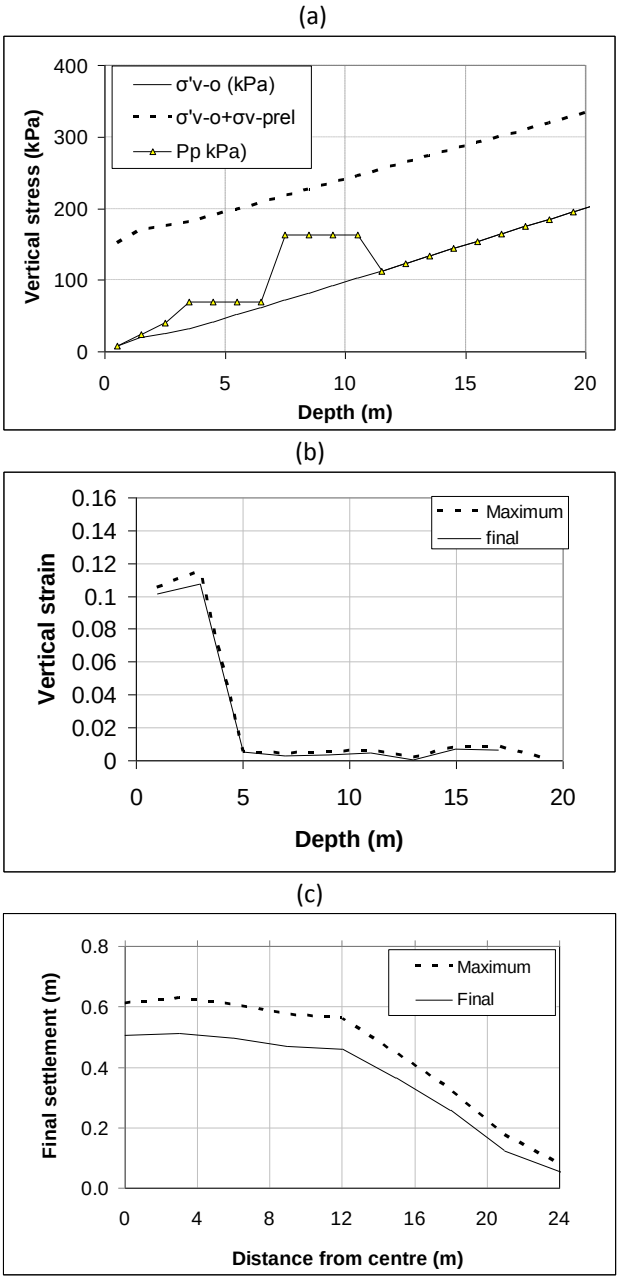

Fig. 2. Porto Romano field test. (a) Initial, maximum and maximum past vertical effective stress versus depth. (b). Maximum and final vertical strain versus depth measured using the magnetic extensiometer, (c) Maximum and final settlement versus location using inclinometer

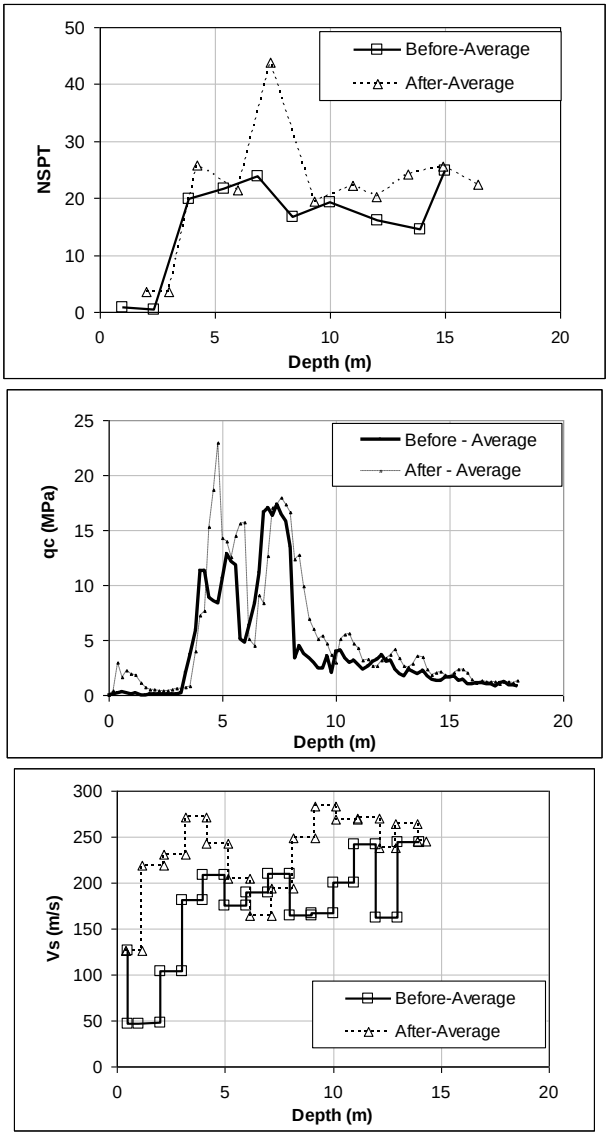

Fig. 3. Porto Romano field test. Average N value of the SPT, qc resistance of the CPT and Vs before and after soil improvement versus depth

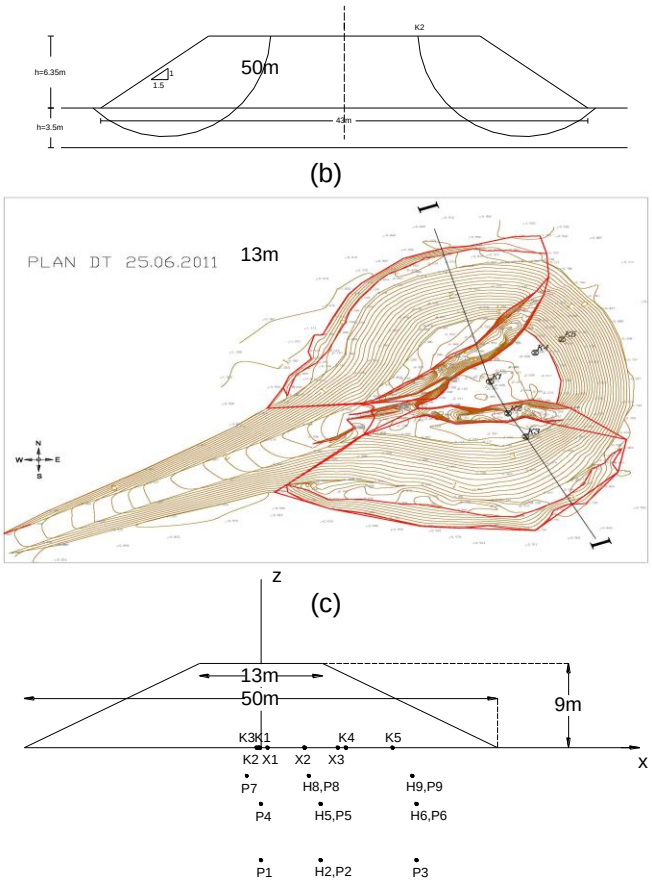

Fig. 4. Porto Romano field test. (a) Schematic illustration of failure, (b) Topographic imprint of the failure. (c) Cross-section of the embankment used for the preloading process. The location of the settlement plates (Xi), vertical pressure cells (Ki), pore pressure transducers (Pi) and horizontal pressure cells (Hi) is also given.

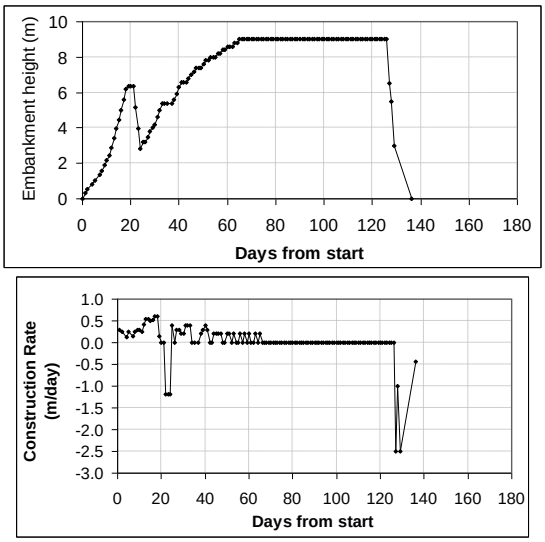

Fig. 5. Porto Romano field test. (a) The height of the embankment (b) the corresponding construction rate.

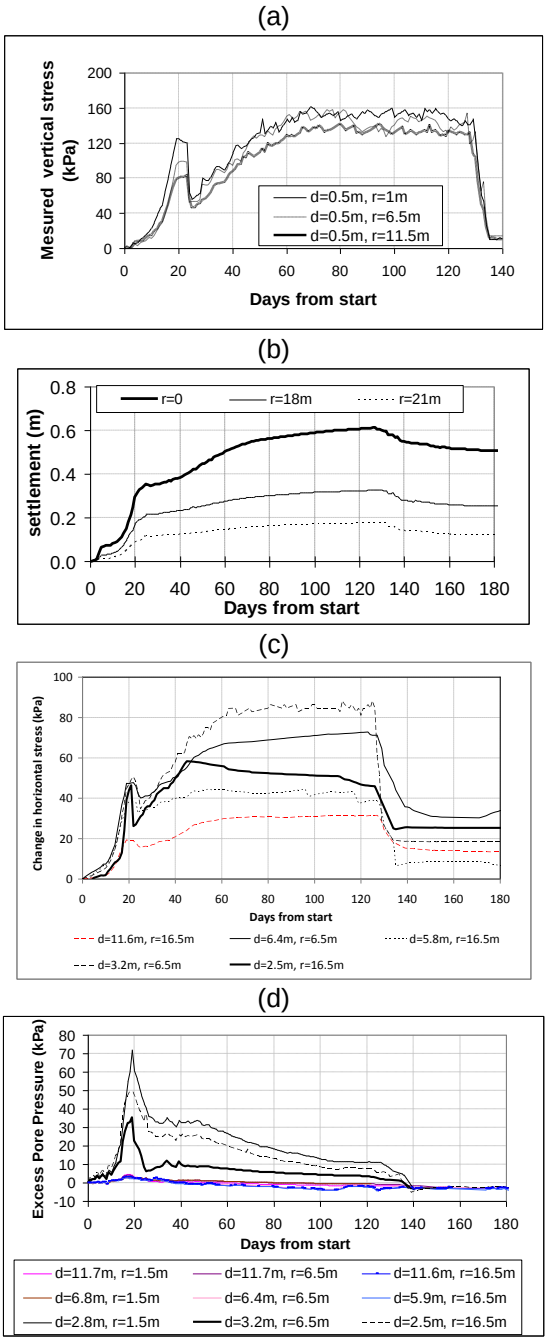

Fig. 6. Porto Romano field test. (a) the measured settlement vertical stresses just below the embankment, (b) the measured settlement at the centerline, (c) the measured effective horizontal stress normalized to have zero initial stress at the locations of the pressure cells and (d) the measured excess pore pressure at the locations of the transducers, all versus the days from the start of construction.

Table 1. Soil layers that exist in the site and their properties based on the geotechnical investigations and relevant laboratory tests.

Layer depth	0-3.5m	3.5-7m	7m-15m
Layer description	Silty Clay	Medium Gravel with silty sand	Fine Sand and Silt
PI	30%	<5%	<5%
Fines content	77	15	95
Cc	0.52	0.05	0.06
Cr	0.02	0.01	0.02
Initial void ratio	1.40	0.58	0.64
Total Density [t/m^3]	1.66	2.02	2.07
Friction angle (for c=0)	28	39	25

Table 2. Average measured N_{SPT} ,qc-CPT and Vs before and after soil improvement Vs in terms of soil layer and corresponding ratio of increase

	Quantity	Depth		
		0-3.7m	3.7-7m	7-15m
Bef. (Pre-improvement)	N_{SPT}	0.6	21.7	20.9
	qc (CPT)	0.4	10.0	4.33
	Vs	94	192	197
After (Post-improvement)	N_{SPT}	3.5	23.6	25.9
	qc (CPT)	1.01	11.8	6.11
	Vs	202	212	246
Ratio	N_{SPT}	6.3	1.1	1.4
	qc (CPT)	2.3	1.2	1.4
	Vs	2.2	1.1	1.2

Table 3. Measured vertical stresses induced by the surcharge at ground level.

Device	Location	$\Delta\sigma_{v-max-m}$: kPa
No	r : m	(a)
1	1.5	160.00
2	6.5	150.00
3	11.5	130.00

Table 4. Measured settlements induced by preloading

Location	Measured	
r : m	δ_{max-m} : m	δ_{res-m} : m
	(a)	(b)
0	0.61	0.51
6.5	0.6	0.48
13	0.5	0.4

Table 5. Increase of horizontal total stress due to the surcharge

Location of measurement			Measured	
No	d : m	r : m	$\Delta\sigma_{h-max-m}$ kPa	$\Delta\sigma_{h-res-m}$ kPa
			(a)	(b)
1	11.6	16.5	32	15
2	6.40	6.5	70	30
3	5.85	16.5	40	9
4	3.25	6.5	85	18
5	2.50	16.5	50	14

Table 6. Measured and predicted increase of liquefaction cyclic strength by preloading

		Depth	
		3.7-7m	7-15m
SR_{15-bef}	N_{SPT}	0.50	0.38
	qc CPT	0.42	-
	Vs	0.39	-
$SR_{15-after}$	N_{SPT}	0.55	0.43
	qc CPT	0.48	-
	Vs	0.46	-
$Rm=SR_{15-after}/SR_{15-bef}$	N_{SPT}	1.10	1.13
	qc CPT	1.14	
	Vs	1.19	
	Ave	1.14	1.19

METHOD PREDICTING RISK OF EMBANKMENT FAILURE DURING CONSTRUCTION

Proposed method

During application of soil improvement by preloading in the field, soil stability failure during the construction of the preload embankment is of considerable concern, especially if the in-situ soil is soft clay: If the construction rate is too fast, considerable excess pore pressures can develop and the undrained soil strength can be mobilized without the increase due to the consolidation induced by the weight of the embankment.

Fig. 6a gives a chart relating the approximate normalized undrained strength for failure in terms of geometry of embankment and the depth of soft layer (Lambe and Whitman, 1969). Referring to Fig. 6a, the undrained failure strength equals (su-fail) approximately equals

$$su_{-fail} \approx A\,\gamma_e\,H \qquad (1)$$

where γ_e is the unit weight of the clay layer and the embankment, H is the height of the embankment and A is a factor that depends on the height and inclination of the embankment.

Soft clays are typically normally consolidated. The undrained soil strength of normally-consolidated soft clay layers, according to common practice in soil mechanics (Ladd et al, 1977) can be estimated, as a first approximation, as

$$su \approx 0.2\ \sigma'v \qquad (2)$$

where σ'v is the in-situ effective vertical stress.

Using equation (1) and (1), it is inferred that the local factor of safety against failure in terms of time and location can be obtained from the pore water pressure as

$$FS_{t-i} \approx A\gamma_e h_t / [0.2\ \sigma'_{v(t-i)}] \approx 5A\ \gamma_e h_t / (\sigma_{v(t-i)} - P_{t-i}) \quad (3)$$

where the subscript t indicates variation in terms of time and the subscript (t-i) indicates variation in terms of location and time.

Equation (3) provides an estimate of the local factor of safety versus time of construction in the case that near the surface the in-situ soil consists of soft clay. When this parameter is near unity, danger of embankment failure exists. Application of equation (3) needs pore pressure measurements, while the total vertical stress can be estimated from solutions of linear elasticity readily available. It is inferred that installation of pore pressure transducers to measure the pore pressures is very important to illustrate risk of failure during preload embankment construction at soft clay layers.

Evaluation

Referring to Fig. 6a, as in the geometry of the field test described above, coti=1.5 and D/H=1.5. Thus, the factor A of equation (1) equals 0.17 and equation (3) becomes

$$FS_{t-i} \approx 0.17\gamma_e h_t / [0.2\ \sigma'_{v(t-i)}] \approx 0.85\ \gamma_e h_t / (\sigma_{v(t-i)} - P_{t-i}) \quad (4)$$

where the subscript t indicates variation in terms of time and the subscript (t-i) indicates variation in terms of location and time.

Equation (3) provides an estimate of the local factor of safety versus time of construction in the case that near the surface the in-situ soil consists of soft clay. When this parameter is near unity, danger of embankment failure exists. Application of equation (3) needs pore pressure measurements, while the total vertical stress can be estimated from solutions of linear elasticity readily available. It is inferred that installation of pore pressure transducers to measure the pore pressures is very important to illustrate risk of failure during preload embankment construction at soft clay layers.

The local factor of safety FSt-i is determined in the locations of the transducers versus time using equation (5) and (i) the total vertical stress estimated by linear elasticity in terms of ht and (b) the measured pore water pressure at the locations of the transducers at the upper clay layer and presented in Fig. 6b. Fig. 6c gives the corresponding vertical effective stress. From Fig. 1b it can be observed that FSt-i (a) has a minimum value in all piezometer locations at the time of failure (or t=18days) and (b) at the piezometers at depths 2.5 and 2.8m is less than or equal to unity. The above illustrate that the measured excess pore pressures are consistent with the failure of the embankment that occurred on day 18. It should be noted that the undrained soil strength predicted by equation (2) and used in equation (3) is also in general agreement with the undrained strength of the upper clay measured in samples retrieved from borings in triaxial tests, considering also soil anisotropy that reduces soil strength by about 15% (Mayne, 1985). Concluding, equation (3) predicts the embankment failure.

DISCUSSION

The field test data presented above can be used to evaluate the accuracy of methods that have been proposed predicting the increase of shear wave velocity and liquefaction cyclic strength with preloading, described in the introduction. In addition, they can be used to correlate the measured increase in density and horizontal stress to the increase of shear wave velocity and liquefaction cyclic strength with preloading. However, these are beyond the scope of the present paper

CONCLUSIONS

An elaborate field study of soil improvement by preloading that was recently performed is described. The site consisted of (a) a soft clay layer to depth of 3.5m, (b) a medium-dense silty sand layer at depths 3.5-7m and (c) a soft silt layer below. Preloading was applied by a temporary embankment 9m high. A partial embankment failure occurred during the preloading process. Preloading caused settlement of about 0.6m with vertical strain ranging from 10% at depths above 3.5m to 1% below. The increase in lateral stress ratio as a result of the preloading process varies between 0.9 and 0.1. The large value corresponds to depths 0-3.7m. As a result of preloading the shear wave velocity increased from a factor of about 2 to a factor of about 1.1. The large value corresponds to depths 0-3.7m. The cyclic liquefaction strength of a silty sand layer at depth 3.7-7m increased from 0.39-0.50 to 0.46-0.55, or by about 10%. In addition the cyclic liquefaction strength of a non-plastic silt layer at depth 7-15m increased from 0.38 to 0.43, or by about 13%.

The paper also presents and verifies method predicting failure during the construction of the preload embankment based on excess pore pressure measurements is proposed and verified.

ACKNOWLEDGEMENT

The work is funded by the Seventh Framework Programme of the European Community, European Commission Research Executive Agency under grant agreement FP7-SME-2010-1-

262161-PREMISERI. Prof. Modaressi and Dr Lopez-Caballero assisted on the interpretation of the field test.

(a)

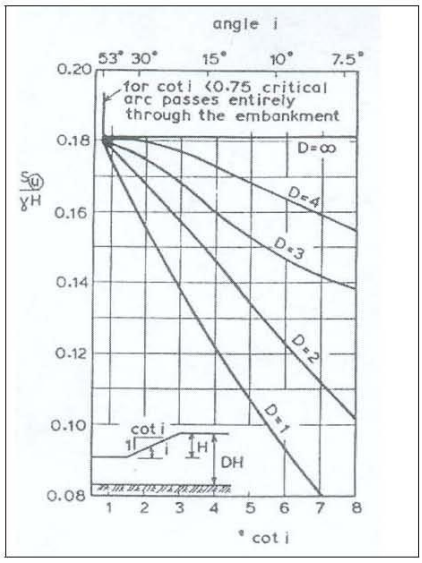

(b1)

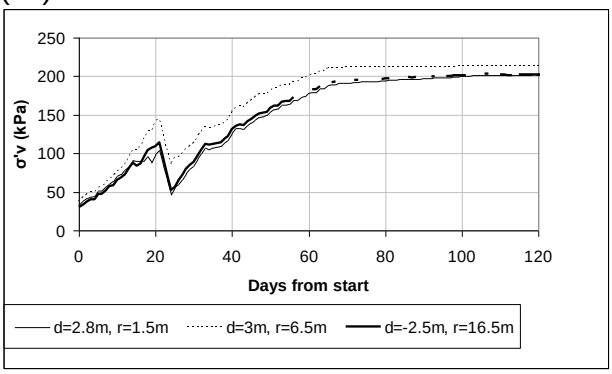

(b2)

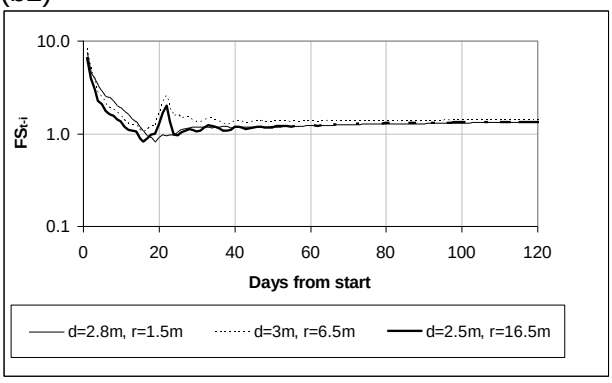

Fig. 6. (a) Stability chart giving the undrained soil strength for embankment failure (Lambe and Whitman, 1969), (b). Porto Romano field test. Effective stress and factor of safety versus time considering the measured pore pressures and using eq. (4).

REFERENCES

Alonso EE, Gens A, Lloret A. (2000). Precompression design for secondary settlement reduction, Geotechnique, 50, No 6, 645-656.

Al-Shamrani Mosleh A, Dhowian Abdulmohsin W. (1997) Preloading for reduction of compressibility characteristics of sabkha soil profiles. Engineering Geology. Volume 48, Issues 1–2, 19 November 1997, Pages 19–41

Boulanger R. W. and Idriss I. M. Liquefaction Susceptibility Criteria for Silts and Clays. the Journal of Geotechnical and Geoenvironmental Engineering, Vol. 132, No. 11, November 1, 2006.

European Prestandard. Eurocode 8 - Design provisions of earthquake resistance of structures, Part 5: Foundations, retaining structures and geotechnical aspects, 1994.

European Standard (2003) Eurocode 8: Design of structures for earthquake resistance, Final Draft, prEN 1998-5, December

Hardin B. O. The nature of stress-strain behavior of soils. Proceedings, Conference on Earthquake Eng. And Soil Dynamics, ASCE, Pasadena, USA, 1978, pp 3-90.

Idriss I. M. and R. W. Boulanger. Semi-empirical procedures for evaluating liquefaction potential during earthquakes. Invited Paper Presented at The Joint 11th International Conference on Soil Dynamics & Earthquake Engineering (ICSDEE) and The 3rd International Conference on Earthquake Geotechnical Engineering (ICEGE), January 7 – 9, 2004, Berkeley, California, USA

Itasca Consulting Group, Inc. Fast Langrangian Analysis of Continua, Use's Guide. Minneapolis, Minessota, USA, 2001.

Ishihara K. Liquefaction and Flow Failure During Earthquakes, 33rd Rankine Lecture, Geotechnique, 1993, Vol. 43, No. 3, pp 351-415.

Ishihara K. and Takatsu H. Effects of overconsolidation and Ko conditions on the liquefaction characteristics of sands. Soils and Foundations, Japanese Society of Soil Mechanics and Foundation Engineering, 1979, 19, No 4, pp 59-68.

Kramer S. L. "Geotechnical earthquake engineering" Prentice Hall, New Jersey, 1996.

Lambe T. W and Whitman R. V. Soil Mechanics, John Wiley and Sons, 1969.

Ladd, C.C., Foot, R., Ishihara K., Schlosser F. & Poulos H.G. 1977. Stress- Deformation and Strength. Characteristics, Proc.9th ICSMFE. Tokyo, 2, : 421-497.

Mayne P. W. and Kulhway F. W. Ko-OCR relationships in Soils. Journal of the Geotechnical Engineering Division, ASCE, 1982, 108, No 6, pp 851-872.

Mayne Paul W. Stress Anisotropy Effects on Clay Strength. Journal of Geotechnical Engineering, Vol. 111, No. 3, March 1985, pp. 356-366

Petridis P., Stamatopoulos C. and Stamatopoulos A. Soil Improvement by preloading of two erratic sites. GeoEng2000, International conference on Geotechnical and Geological Engineering, Melbourne, Australia, 2000. (in CD-ROM)

Raptakis D. G. Pre-loading effect on dynamic soil properties: Seismic methods and their efficiency in geotechnical aspects. Soil Dynamics and Earthquake Engineering. Volume 34, Issue 1, March 2012, Pages 69–77

Seed, H. B., and De Alba, P. (1986), " Use of SPT and CPT Tests for Evaluating the Liquefaction
Resistance of Sands." Proc. of the ASCE Specialty Conf. In-Situ'86: Use of In-Situ Tests in
Geotechnical Engineering, Blacksburg, 281-302

Schnabel, P. B., Lysmer J. and Seed H. B. SHAKE: A computer program for earthquake response analysis of horizontally layered sites. Report No. EERC 72-12. Earthquake Engineering Research Centre, University of California, Berkeley, California, 1972.

Stamatopoulos A. C., Kotzias P. C. Soil improvement by preloading. J. Wiley & Sons Publications, 1985.

Stamatopoulos C. Petridis P., Bassanou M., Stamatopoulos A. (2005) "Increase in horizontal stress induced by preloading" Ground Improvement, 9 (2), pages 47-58.

Stamatopoulos, C.A, Lopez-Caballero F., Modaressi-Farahmand-Razavi A. (2012), Laboratory tests and numerical simulations giving the effect of preloading on the cyclic liquefaction strength, 15WCE, Losboa, Portugal

Stamatopoulos C., A., Stamatopoulos A. C. (2007) Effect of preloading on the cyclic strength of reconstituted sand. Journal of Ground Improvement, Thomas Telford Ltd, Volume 11, Number 3, July. 145-155

Wood D. M. Soil behaviour and critical state soil mechanics. Cambridge: Cambridge University press, 1990.

Whittle A. J. and Kavvadas M. J. Formulation of MIT-E3 constitutive model for overconsolidated clays. Journal of Geotechnical Engineering, ASCE, 1994, 120, No 1, pp 173-198.